Supporting Information for

ORIGINAL ARTICLE

In situ tumor vaccine with optimized nanoadjuvants and lymph node targeting capacity to treat ovarian cancer and metastases

Yuan Li[a,†], Fan Tong[b,†], Yufan Wang[b], Jing Wang[b], Manqi Wu[a], Hanmei Li[c], Hongyan Guo[a,*], Huile Gao[b,*]

[a]*Department of Obstet Gynecol, Peking University Third Hospital, Beijing 100191, China*

[b]*Key Laboratory of Drug Targeting and Drug Delivery Systems, West China School of Pharmacy, Sichuan University, Chengdu 610041, China*

[c]*School of Food and Biological Engineering, Chengdu University, Chengdu 610106, China*

Received 22 January 2024; received in revised form 17 April 2024; accepted 20 April 2024

[*]Corresponding authors.

E-mail addresses: bysyghy@163.com (Hongyuan Guo), gaohuile@scu.edu.cn (Huile Gao).

[†]These authors made equal contributions to this work.

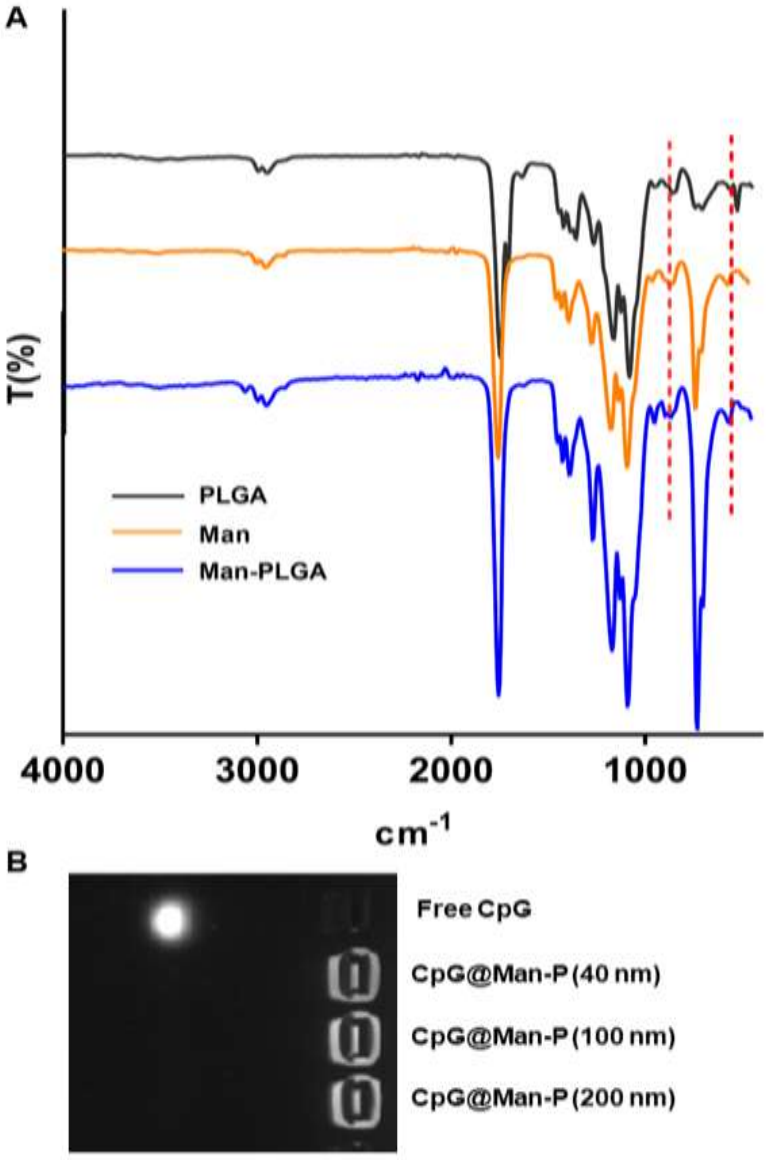

Figure S1 (A)FT-IR spectrum of PLGA, Man, and Man-PLGA. (B) Characterization of CpG@Man-P loaded with CpG by agarose gel electrophoresis (40, 100, 200 nm).

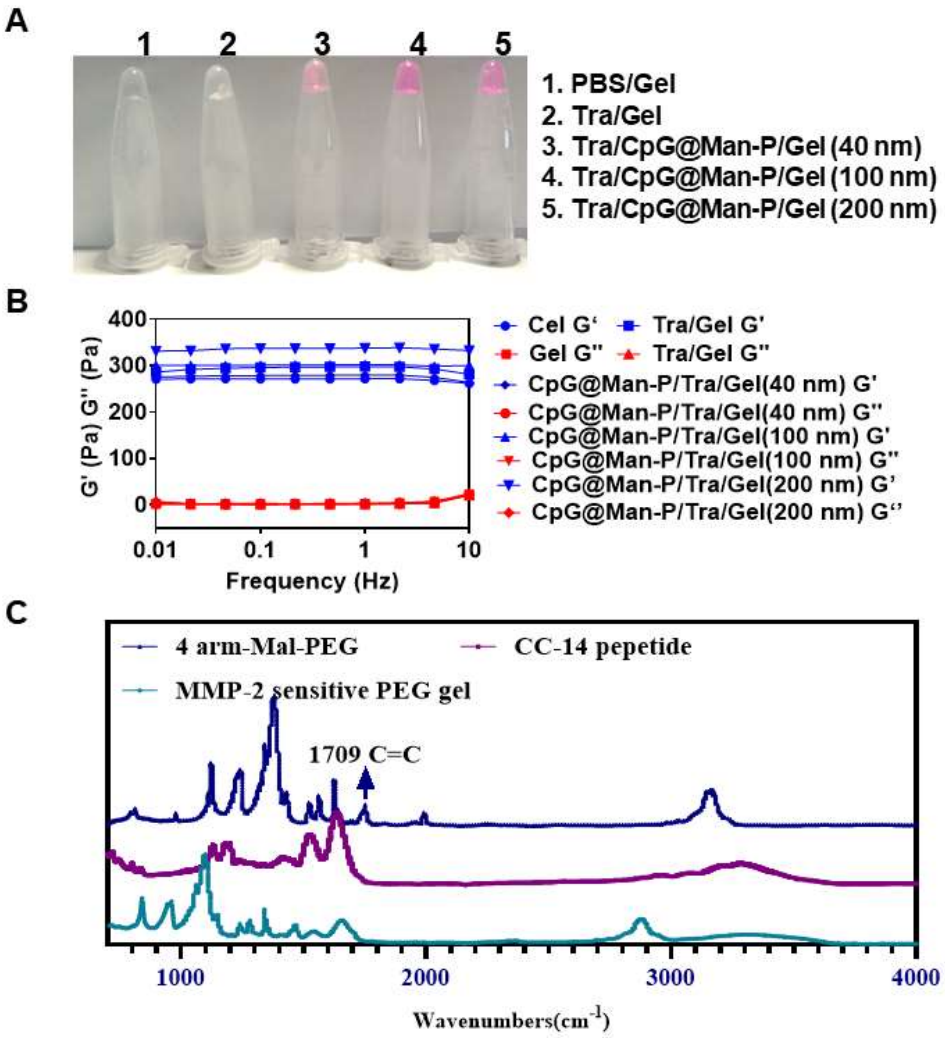

Figure S2 (A) Inversion method to characterize hydrogels. (B) Rheological properties of hydrogels. (C) FT-IR characterization of hydrogels.

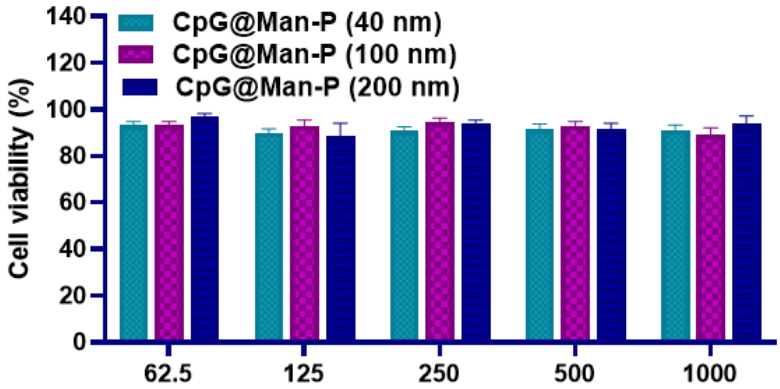

Figure S3 MTT assay of CPG@Man-P (40 nm, 100 nm, 200 nm) on DC2.4. cells. Error bars represent mean ± SD (n = 4).

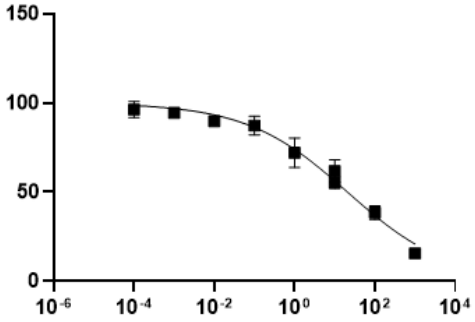

Figure S4 MTT assay of Tra on ID8 cells.

-

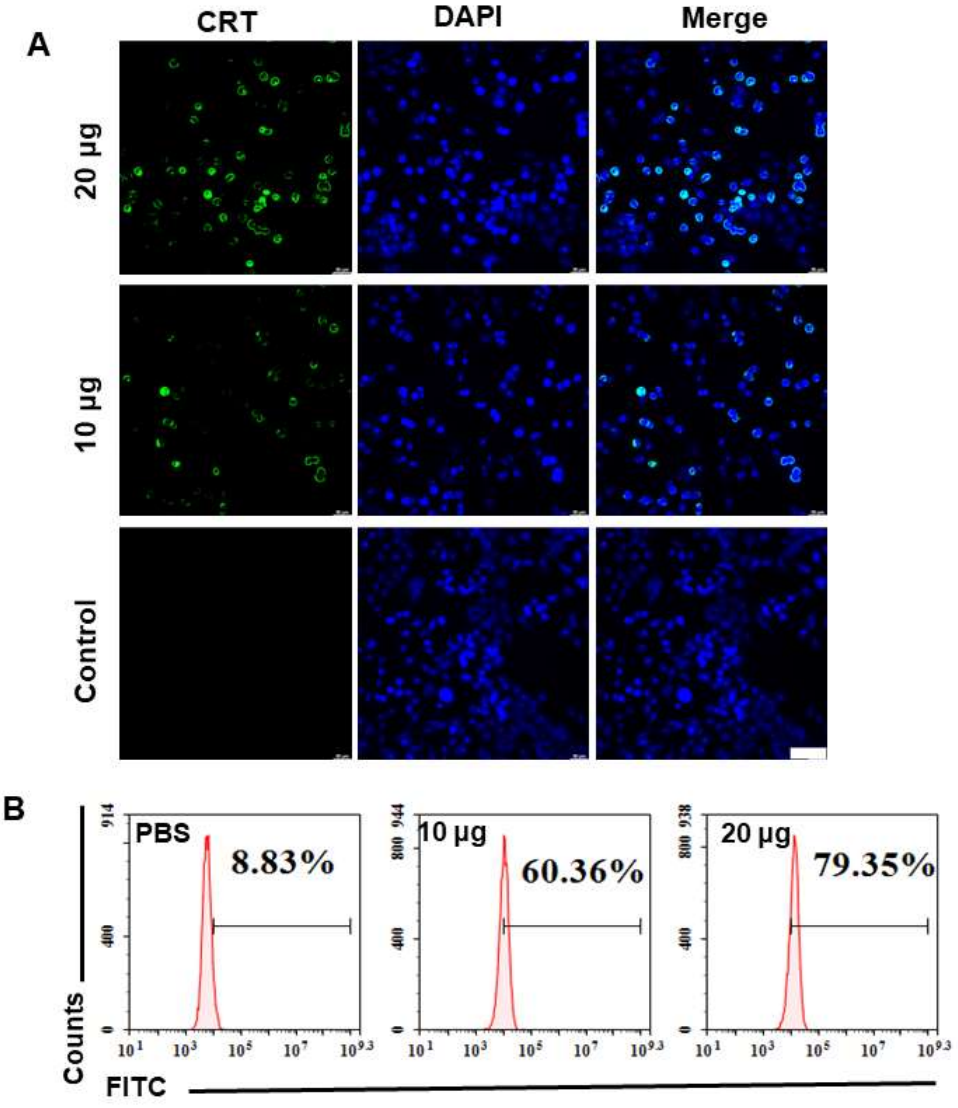

Figure S5 (A, B) Confocal (A) and flow cytometry (B) characterization of CRT exposure on the surface of ID8 cells. The scale bars represent 50 μm.

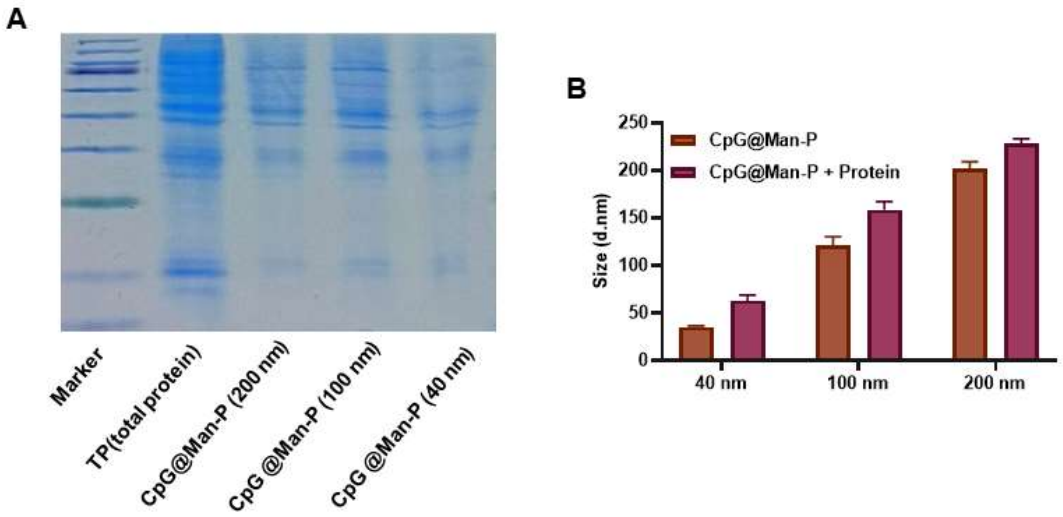

Figure S6 (A) SDS-PAGE characterization of antigen adsorption on CPG@Man-P (40 nm, 100 nm, 200 nm). (B) Size change of CPG@Man-P (40 nm, 100 nm, 200 nm) after antigen absorption. Error bars represent mean ± SD (*n* = 3).

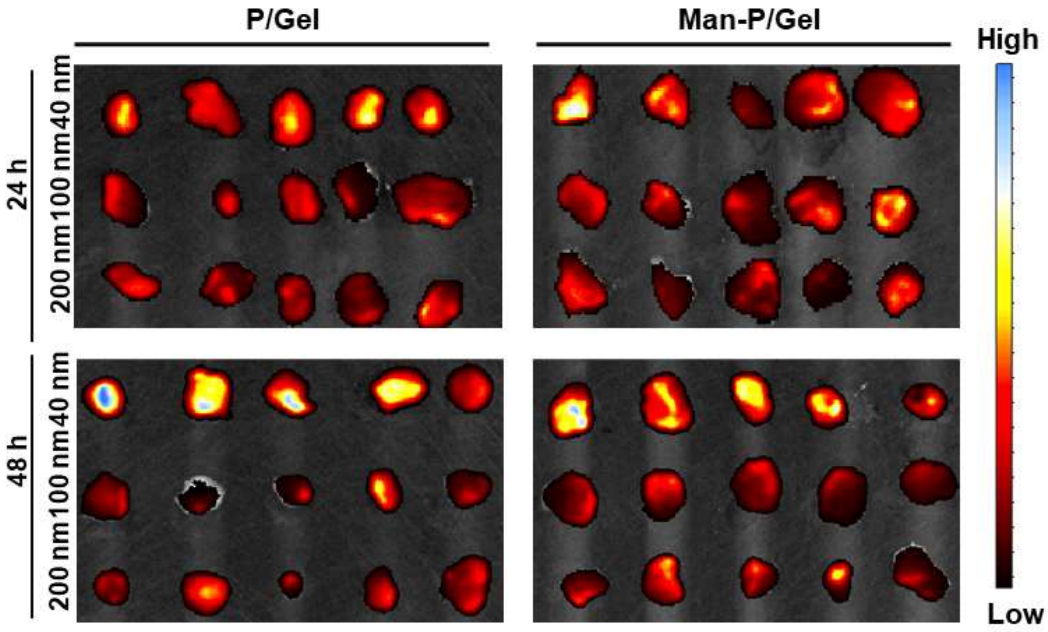

Figure S7 DiR@Man-P (40 nm, 100 nm, 200 nm) accumulation at the tumor site.

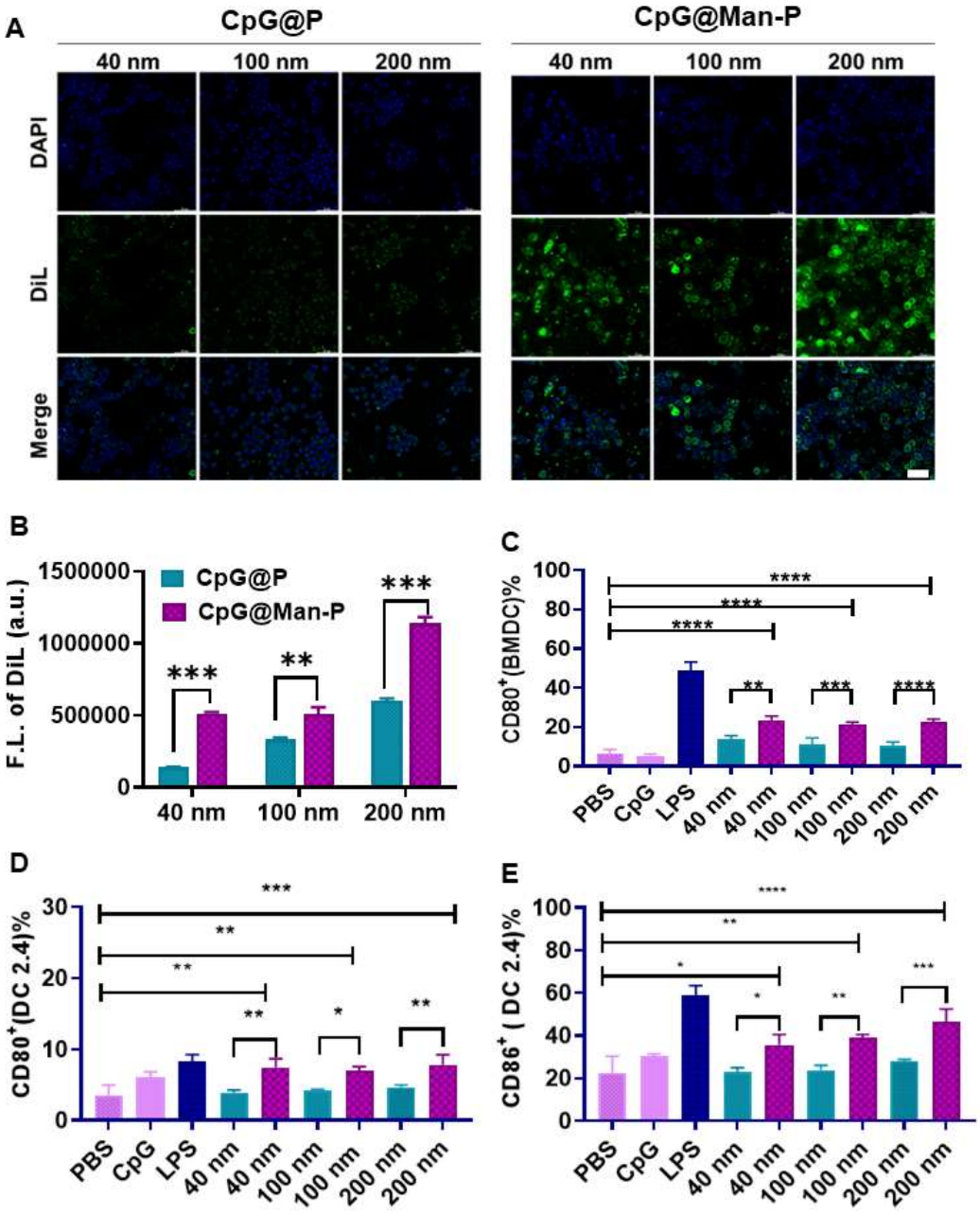

Figure S8 (A) Cellular uptake of Dil@P and Dil@Man-P by DC2.4 cells, which was observed by confocal microscope. The scale bar represents 50 μm. (B) Cellular uptake of Dil@P and Dil@Man-P by DC2.4 cells. (C) Percentages of $CD80^+$ BMDC cells gated by $CD11c^+$. Percentages of $CD80^+$ (D) and $CD86^+$ (E) DC2.4 cells gated by $CD11c^+$. Error bars represent mean ± SD (n = 3). Statistical significance was set at *P < 0.05, ** P < 0.01, *** P < 0.001, **** P < 0.0001, and ns, not significant.

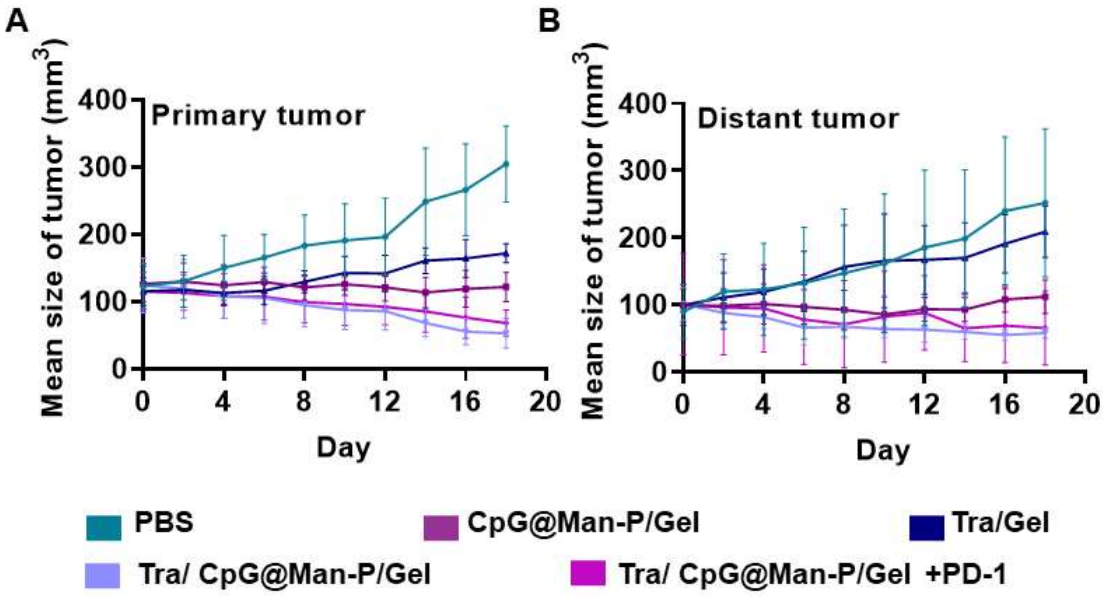

Figure S9 Primary (A) and Distant (B) tumor volume growth curves. Error bars represent mean ± SD (n = 5).

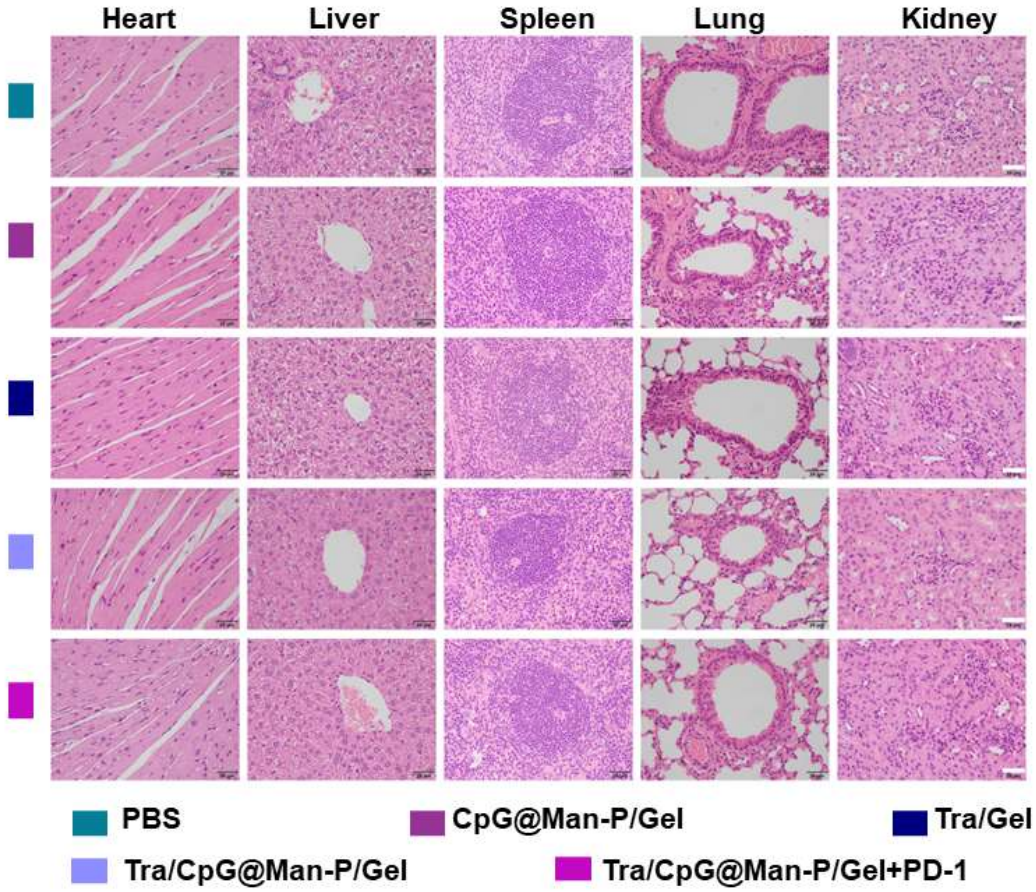

Figure S10 HE imaging of major organs. The scale bars represent 20 μm.

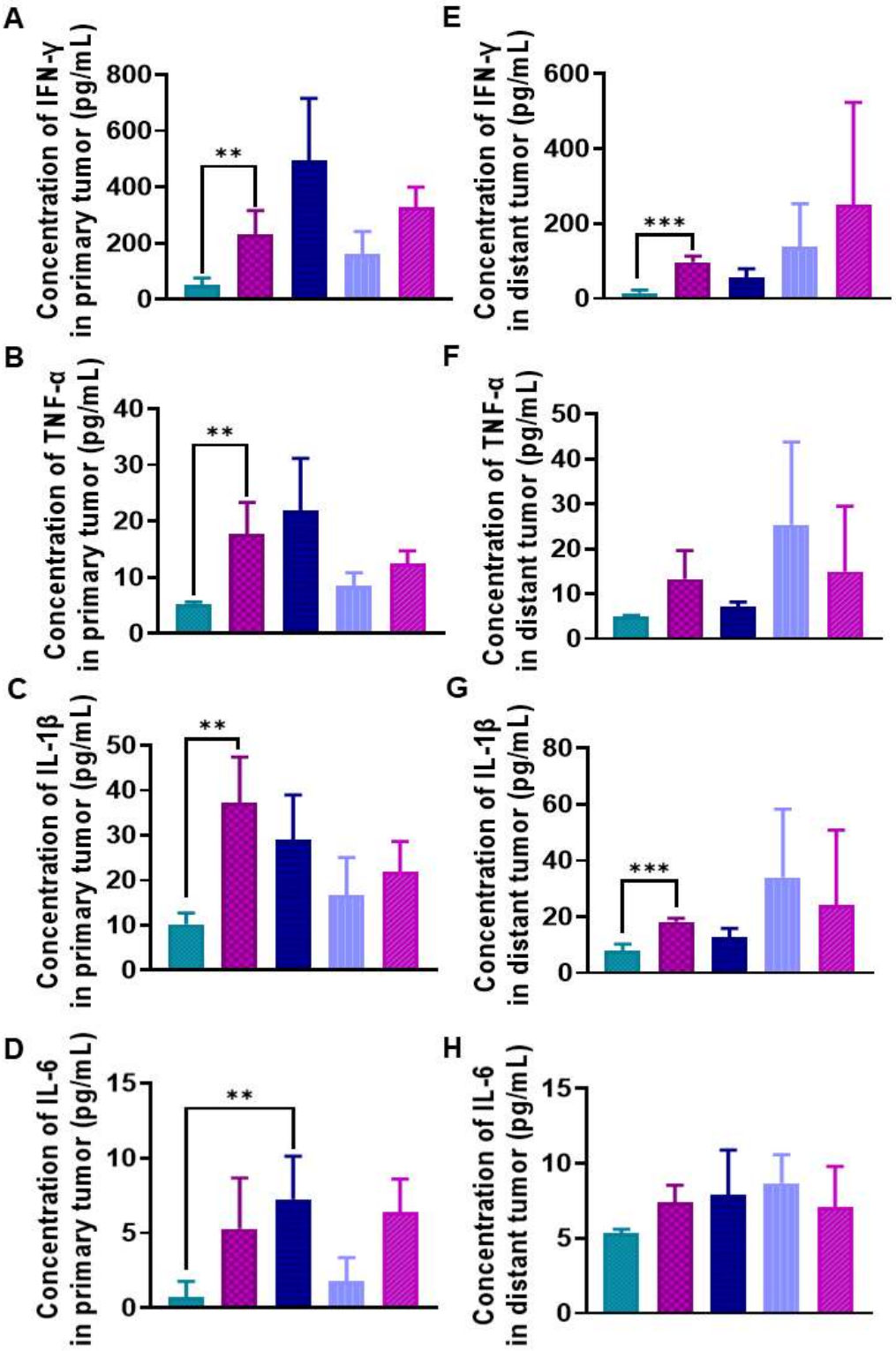

Figure S11 (A-D) Elisa analyses of IFN-γ (A), TNF-α (B), IL-1β (C), and IL-6 (D) levels in the primary tumors. (E-H) Elisa analyses of IFN-γ (E), TNF-α (F), IL-1β (G), and IL-6 (H) levels in the distant tumors. Error bars represent mean ± SD (n = 3, 4).

Statistical significance was set at *P < 0.05, ** P < 0.01, *** P < 0.001, **** P < 0.0001, and ns, not significant.

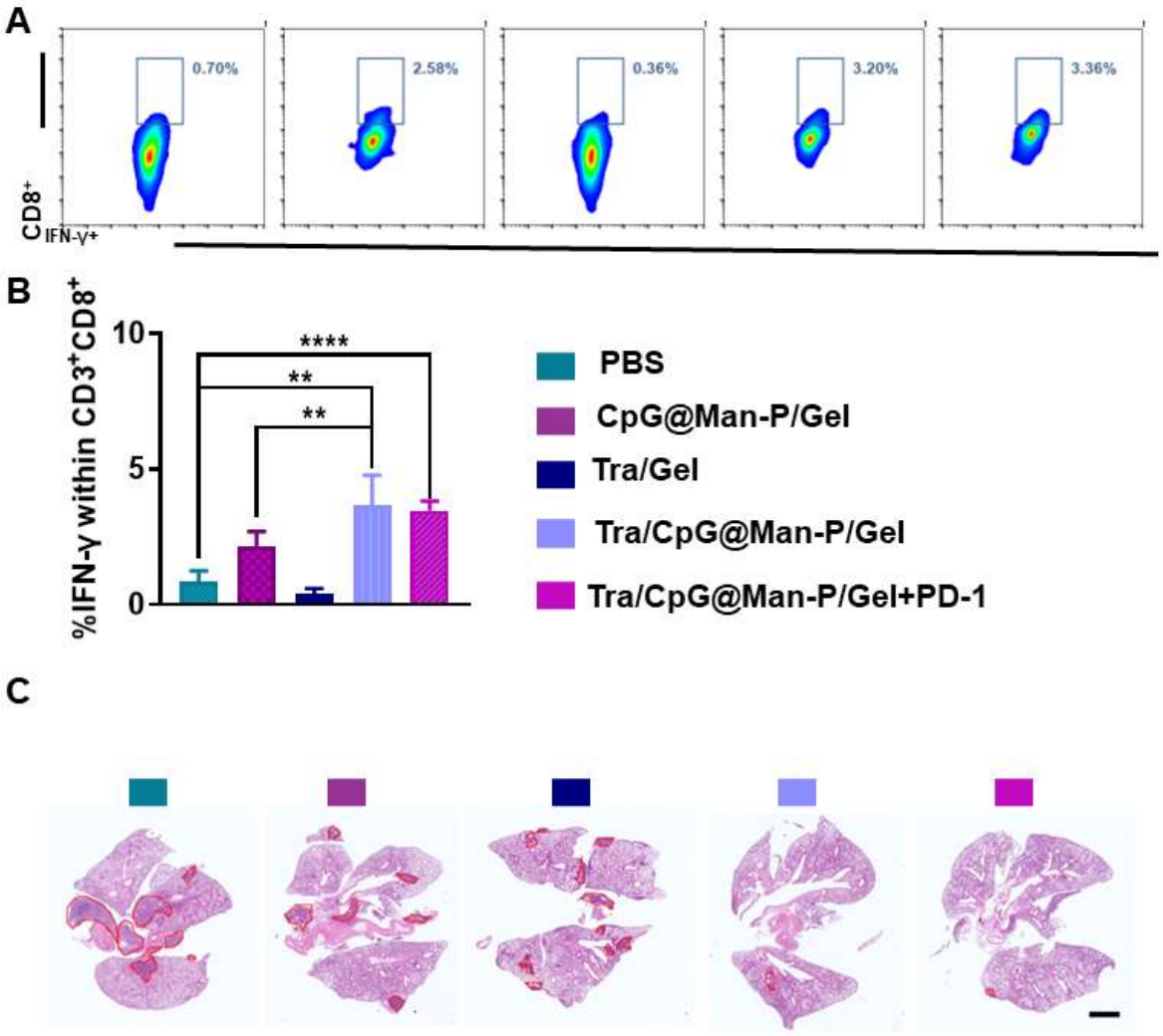

Figure S12 (A, B) The percentage of IFN-γ^+ CD8$^+$ T cells in the primary tumors detected by flow cytometry. (C)HE staining of lung tissues to investigate the anti-metastasis effect. The circled portions were metastatic tumor cells. The scale bar represents 2 mm. Error bars represent mean ± SD (n = 3, 4). Statistical significance was set at *P < 0.05, ** P < 0.01, *** P < 0.001, **** P < 0.0001, and ns, not significant.

Table S1. Drug loading ratio and entrapment ratio of CpG@Man-P

Nanocarrier	Entrapment ratio（%）	Drug loading ratio（%）
CpG@Man-P (40 nm)	77.2 ± 10.3	0.077 ± 0.010
CpG@Man-P (100 nm)	79.2 ± 13.2	0.079 ± 0.014
CpG@Man-P (200 nm)	77.9 ± 14.3	0.079 ± 0.014

Error bars represent mean ± SD (n = 3).